

#### IV. 研究成果の刊行物・別刷

# Gene-expression phenotypes for vascular invasiveness of hepatocellular carcinomas

Shinji Tanaka, MD, PhD, FACS,<sup>a,b</sup> Kaoru Mogushi, PhD,<sup>b</sup> Mahmut Yassen, MD, PhD,<sup>a,b</sup> Norio Noguchi, MD, PhD,<sup>a</sup> Atsushi Kudo, MD, PhD,<sup>a</sup> Noriaki Nakamura, MD, PhD,<sup>a</sup> Koji Ito, MD, PhD,<sup>a</sup> Yoshio Miki, MD, PhD,<sup>c</sup> Jobji Inazawa, MD, PhD,<sup>c</sup> Hiroshi Tanaka, PhD,<sup>b</sup> and Shigeki Arii, MD, PhD,<sup>a</sup> Tokyo, Japan

**Background.** Gross vascular invasion is a well-established prognostic indicator in hepatocellular carcinoma (HCC), but the biological significance of microscopic invasion remains unclear.

**Methods.** Curatively resected primary HCCs were classified retrospectively into 3 groups: HCCs without vascular invasion (V0), HCCs with microvascular invasion (V1), and HCCs with macrovascular invasion (V2). Microarray profiling of patients with V0, V1, and V2 using Jonckheere-Terpstra (JT) tests and Wilcoxon rank sum tests was performed.

**Results.** Distinct patterns of gene expression were demonstrated between V0 and V2 groups; less (L) and highly (H) invasive phenotypes, respectively. It is noteworthy that 2 dendrograms by the hierarchical clustering provided exactly the same assignment results for V1 cases that were thus separated into L and H gene-expression phenotypes. Marked differences were found in overall ( $P < .001$ ) and tumor-free survival ( $P < .001$ ) between L and H gene-expression phenotypes. Multivariate analyses indicated that the phenotypes of the patterns of gene expression, rather than the clinicopathologic markers of vascular invasion, were independent predictors of tumor recurrence ( $P = .031$ ). Using the gene-expression patterns identified by both JT and Wilcoxon rank sum test analyses, other V1 cases validated these differences in tumor-free survivals between gene-expression phenotypes within the group ( $P = .039$ ).

**Conclusion.** Gene profiling suggested that microvascular invasiveness consisted of a classable mixture of 2 distinct phenotypes. Thus, gene-array analyses may have clinical benefit, because they may in fact be more predictive than other clinical factors. (Surgery 2010;147:405-14.)

From the Department of Hepato-Biliary-Pancreatic Surgery,<sup>a</sup> the Information Center for Medical Sciences,<sup>b</sup> and the Medical Research Institute,<sup>c</sup> Tokyo Medical and Dental University, Tokyo, Japan

HEPATOCELLULAR CARCINOMAS (HCCs) are common malignancies, and their prevalence is increasing on a worldwide basis.<sup>1,2</sup> Although operative resection is an effective treatment modality for HCC, the recurrence of these aggressive neoplasms is frequent even after an apparent curative resection.<sup>2,3</sup> The long-term outcome is affected mainly by

metastatic recurrences.<sup>4</sup> Because malignant vascular invasion is regarded as the direct etiology of metastatic recurrences, gross and radiologic evidence suggests that tumor invasion in major veins is a known determinant of poor outcomes after resection of HCC.<sup>5,6</sup> In contrast to visually evident macrovascular invasion in major portal or hepatic veins, microvascular invasion, which is defined as microscopic tumor invasion into smaller intrahepatic vessels as identified on histopathologic analysis, is difficult to determine in preoperative assessments.<sup>7,8</sup> Although macroscopic vascular invasion is an established prognostic indicator and represents a variable in the pathologic staging of HCCs,<sup>8</sup> the biologic significance of microscopic vascular invasion in subjects with resectable HCCs remains obscure.

Genome-wide gene-expression analyses by microarrays offer a potentially important, systematic approach to unfold comprehensive information regarding (gene) transcription profiles.<sup>9</sup>

Supported by Special Coordination Funds for Promoting Science & Technology (Japan Science & Technology Agency) and a Grant-in-Aid from the Ministry of Education, Culture, Sports, Science and Technology of Japan. S.T. is a recipient of the Japan Cancer Society Incitement Award and the Japan Society for the Promotion of Science Prize.

Accepted for publication September 29, 2009.

Reprint requests: Shinji Tanaka, MD, PhD, FACS, Department of Hepato-Biliary-Pancreatic Surgery, Graduate School of Medicine, Tokyo Medical and Dental University, 1-5-45 Yushima, Bunkyo-ku, Tokyo 113-8519, Japan. E-mail: shinji.msrg@tmd.ac.jp. 0039-6060/\$ - see front matter

© 2010 Mosby, Inc. All rights reserved.

doi:10.1016/j.surg.2009.09.037

Furthermore, such studies may lead potentially to the development of novel, molecular-targeting therapies in HCCs.<sup>10</sup> We analyzed previously HCC gene-expression profiles<sup>11</sup> and identified a novel molecule as a therapeutic target. Our current study seeks to identify signatures associated with vascular invasion in HCC from genome-wide expression profiles of HCC as generated from microarray studies. The clinicopathologic features and candidate molecular pathogeneses were evaluated in subjects with HCC with a special emphasis on the significance of tumor vascular invasion.

## SUBJECTS AND METHODS

**Subjects and tissue samples.** All 188 subjects had curative hepatectomies to treat HCC from 2001 to 2006 at the Tokyo Medical and Dental University Hospital. Written informed consent was obtained from each subject, and study procedures were approved by the Institutional Review Board. Pre-operative evaluations, including liver function tests and operative procedures, are described elsewhere.<sup>2,3,11</sup> Pre-operative imaging for tumor staging included abdominal ultrasonography, computed tomography (CT), hepatic arteriography, indirect arterial portography, CT-arteriography, CT-arterial portography, and magnetic resonance imaging (MRI). Radiologic vascular invasion indicated by the presence of tumor thrombi in major branches of portal or hepatic veins was evaluated comprehensively. Intra-operative ultrasonography was performed on all subjects. Resected tissues lacking necrosis were divided into 2 specimens immediately after operation; 1 specimen was snap frozen in liquid nitrogen and stored at  $-80^{\circ}\text{C}$  for microarray analyses, and the other was fixed in 10% formaldehyde solution and embedded in paraffin for histopathologic analysis by a pathologist.

The evidence of portal/hepatic vein tumor invasion was evaluated both macroscopically and microscopically. Gross examinations of resected specimens confirmed the preoperative diagnosis of macroscopic invasion in all examined cases. On histopathologic examinations of resected specimens, microscopic invasion indicated the presence of clusters of cancer cells floating in the vascular space. Radiologically, macroscopic invasion was detected in 45 cases (V2); 47 cases were diagnosed as microscopic vascular invasion on histopathologic analyses (V1), and the remaining 96 cases had no vascular invasion by either macroscopic or microscopic examinations (V0). Subjects were assayed for serum levels of alpha-fetoprotein

(AFP) and protein induced by vitamin K absence or antagonists-II (PIVKA-II) every month and with ultrasonography, CT, and MRI every 3 months. When tumor recurrence was suspected, diagnostic imaging was performed using a CT-angiography. Finally, the diagnosis of a recurrence was made via imaging. The mean observation time was 3.8 years.

**RNA isolation, complementary RNA (cRNA) preparation, and microarray hybridization.** Total RNA was extracted from HCC specimens using an RNeasy kit (Qiagen, Hilden, Germany). The integrity of the obtained RNA was assessed using an Agilent 2100 BioAnalyzer (Agilent Technologies, Palo Alto, CA). All samples had an RNA Integrity Number greater than 5.0. Contaminant DNA was removed by digestion with RNase-free DNase (Qiagen). Using 2  $\mu\text{g}$  total RNA, cRNA was prepared using 1-cycle target labeling and control reagents kit (Affymetrix, Santa Clara, CA). Hybridization and signal detection of HG-U133 Plus 2.0 arrays (Affymetrix) were performed as per the manufacturer's instructions.

**Normalization and statistical analyses of microarray data.** In the 188 cases, 59 were selected randomly for test analyses (V0 = 29 cases, V1 = 14 cases, and V2 = 16 cases), and another 129 cases were evaluated for validation analyses (V0 = 67 cases, V1 = 33 cases, and V2 = 29 cases). Statistical differences were not identified when clinicopathologic factors were analyzed between test and validation cases. Microarray data sets were normalized using a robust multiarray average method under R 2.4.1 statistical software together with a Bioconductor package, as previously described.<sup>11</sup> Estimated gene-expression levels were  $\log_2$ -transformed, and 62 control probe sets were removed for subsequent analyses. For each of the 54,613 probes on the HG-U133 Plus 2.0 array, fold-change (FC) values were calculated using ratios of geometric means of gene-expression levels between subtypes, and genes with an FC difference greater than 1.2-fold were selected for evaluation, according to a previous report.<sup>12</sup> To identify the genes associated with the development of vascular invasion in V0, V1, and V2 cases, we applied Jonckheere-Terpstra (JT) tests, which are nonparametric tests for monotone trends in terms of ordinary classes.<sup>12</sup> In addition, Wilcoxon rank sum tests were performed to estimate the significance levels of gene-expression differences between V0 and V2 groups for each of the 54,613 probe sets. For each statistical test, obtained *P* values from multiple hypothetical tests were adjusted by a false discovery rate (FDR), and probe sets with a FDR  $<5\%$  were considered for subsequent analysis.

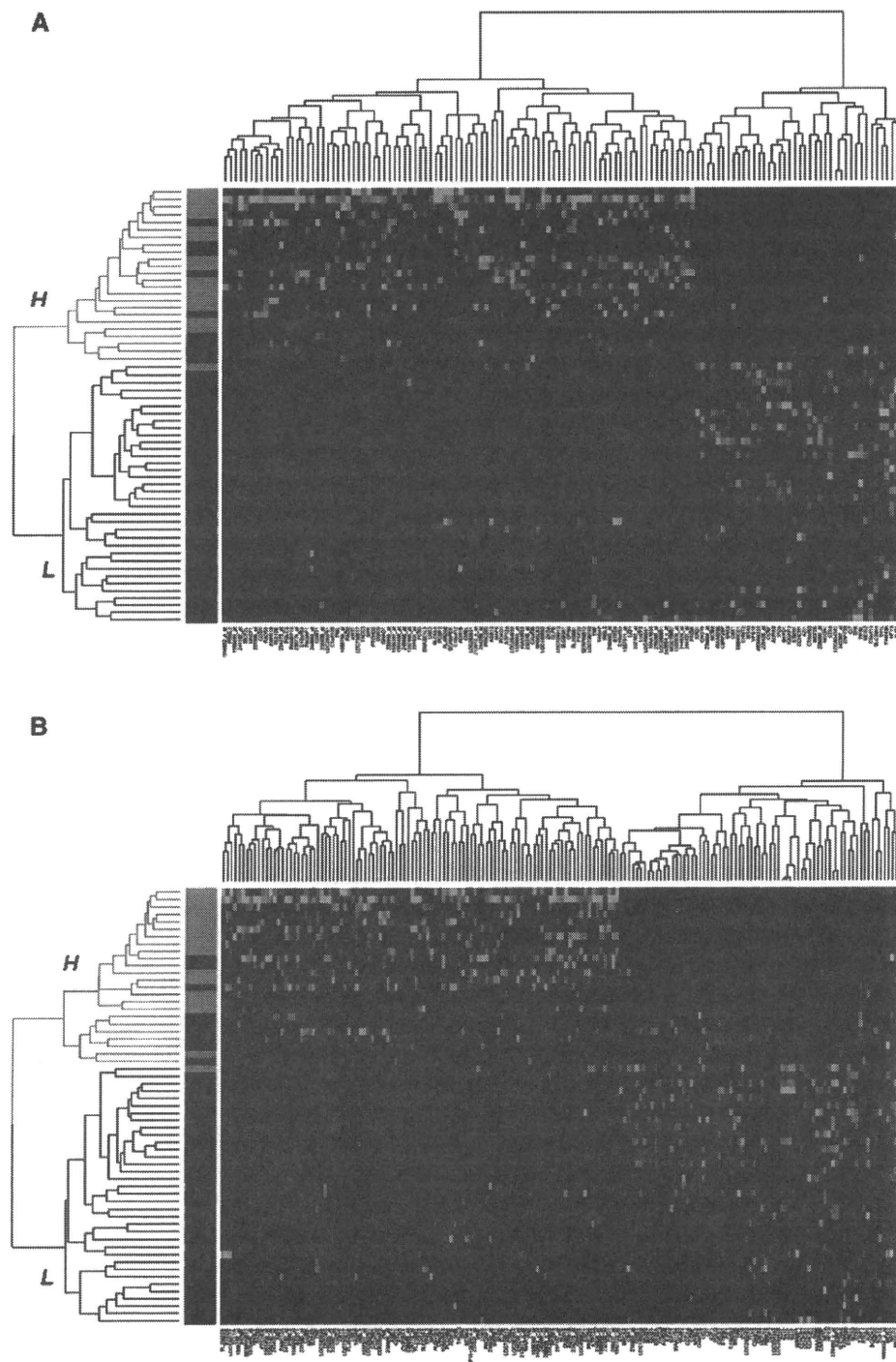


**Fig 1.** Hierarchical clustering of gene-expression profiles on 59 HCC subjects; 29 with no vascular invasion (V0: black bar), 14 with microvascular invasion (V1: blue bar), and 16 with macrovascular invasion (V2: orange bar). Dendrograms shows the classification determined by hierarchical clustering analyses; less (L) and highly (H) invasive phenotypes. Red and green colors indicate relative overexpression and underexpression, respectively. (A) Hierarchical clustering with 132 probe sets, which showed monotone trends with the development of vascular invasion in V0, V1, and V2 cases (JT tests; Supplementary Table I). (B) Hierarchical clustering using 172 probe sets, which were differentially expressed in V0 and V2 cases (Wilcoxon rank sum test; Supplementary Table II).



**Table I.** Comparison of the clinicopathologic factors between gene-expression phenotypes

| Variables                                  | L phenotype (n = 37) | H phenotype (n = 22) | P value |
|--|----------------------|----------------------|---------|
| Age (>65 years)                            | 22:15                | 12:10                | .712    |
| Sex (male:female)                          | 27:10                | 17:5                 | .714    |
| Hepatitis virus (HBV:HCV:None)             | 9:15:13              | 7:11:4               | .379    |
| Child-Pugh (A:B:C)                         | 35:2:0               | 21:1:0               | .999    |
| ICG-R15                                    | 18.3 ± 2.3           | 19.2 ± 2.6           | .804    |
| Number of neoplasms                        | 1.3 ± 0.1            | 1.6 ± 0.2            | .099    |
| Size of neoplasm                           | 3.6 ± 0.4            | 6.2 ± 1.2            | .022    |
| Histologic differentiation (well:mod/poor) | 12:25                | 0:22                 | .002    |
| Growth pattern (expansive:invasive)        | 36:1                 | 20:2                 | .549    |
| Capsular formation (+:-)                   | 27:10                | 17:5                 | .714    |
| Capsular invasion (+:-)                    | 19:18                | 16:6                 | .106    |
| Biliary invasion (+:-)                     | 1:36                 | 2:20                 | .549    |
| Systematized hepatectomy (+:-)             | 29:8                 | 20:2                 | .295    |
| AFP (>100 mAU/mL)                          | 10:27                | 15:7                 | .002    |
| PIVKA-II (>300 mAU/mL)                     | 12:25                | 13:9                 | .045    |

Hierarchical clustering with selected genes was performed on R software using the Pearson correlation coefficient as a similarity index and a complete linkage method for agglomeration. For visualization, expression intensities were standardized by z scores (mean = 0 and variance = 1) for each probe set. Biomolecular network interaction analyses were performed using databases such as BIND and KEGG, as described previously.<sup>12</sup>

**Immunohistochemical analyses.** To validate expression patterns detected by microarrays, immunohistochemical studies were performed on 89 HCC samples. Tissue sections were stained using anti-AURKB antibodies (ab2254; Novus Biologicals Inc., Littleton, CO) at 1:50 dilutions with phosphate buffered solution (PBS) containing 1% bovine serum albumin (Sigma, St. Louis, MO),<sup>11</sup> followed by reactions in an automated immunostainer (Ventana XT System; Ventana, Tucson, AZ) using heat-induced epitope retrieval and a standard DAB detection kit (Ventana). Strong, diffuse, nuclear staining in >10% of cells was considered a positive result. The immunohistochemical staining was evaluated under a light microscope by 2 independent investigators.

**Statistical analyses.** Statistical comparisons of clinicopathologic characteristics for significance were made using Chi-square tests or the Fisher exact tests with a single degree of freedom, and Student *t* tests were used to analyze differences between continuous values. Cumulative survival and recurrence rates were determined using the Kaplan-Meier method, and for comparisons, we used log-rank tests. *P* values of <.05 were considered statistically significant.

## RESULTS

**Gene-expression analyses of vascular invasion.** The molecular properties of cases with vascular invasion were analyzed in 59 test cases composed of V0 (*n* = 29), V1 (*n* = 14), and V2 (*n* = 16). Microarray analyses of changes in gene expression among V1, V1, and V2 groups revealed that 132 probe sets showed strong monotone trends with the development of vascular invasion at FDR <5% (*P* < .0001) by JT tests (see Supplementary Table I in the online version at doi: 10.1016/j.surg.2007.09.037, published on the electric version only). Similarly, by evaluating changes in gene expression between V0 and V2 groups, 172 probe sets that satisfied FDR <5% (*P* < .0001) with Wilcoxon rank sum tests were identified as differently expressed genes (see Supplementary Table II in the online version at doi: 10.1016/j.surg.2007.09.037).

Hierarchical clustering using selected probe sets are shown in Fig 1, A and (JT tests) B (Wilcoxon rank sum tests). Both analyses revealed that all but 1 of the V0 and V2 cases were divided clearly into 2 major clusters: A less (L) invasive phenotype (L) and a highly (H) invasive phenotype of gene expression. No cluster was evident within the V1 cases analyzed. It is noteworthy that the 2 dendrograms identified by the hierarchical clustering provided exactly the same assignment results for 14 V1 cases that were thus classified into the following 2 subtypes (Fig 1, A and B): 6 V1-cases located in the middle of a V0 cluster were denoted as the L phenotype, and the remaining 8 V1-cases located in the V2 cluster were denoted as the H phenotype.

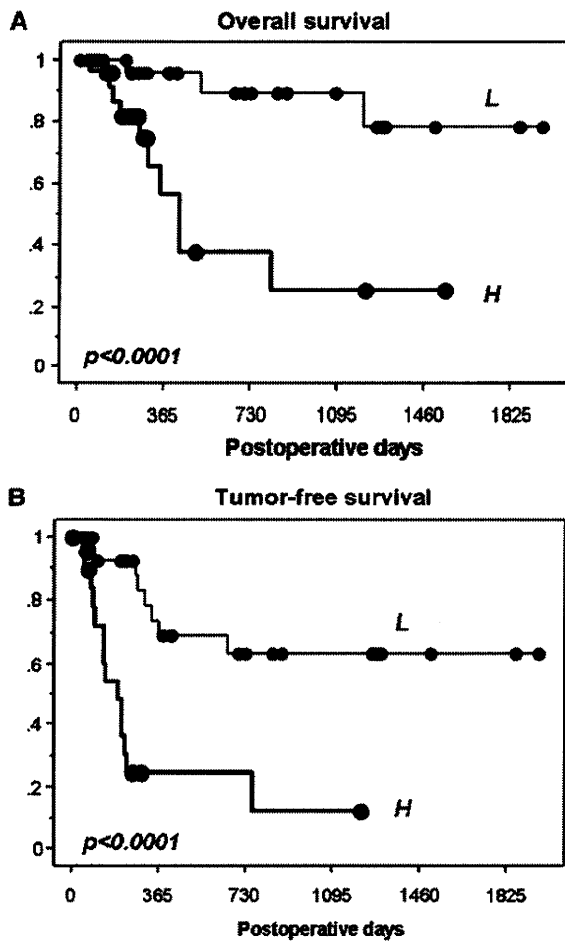


Fig 2. Cumulative overall survival curves (A) and tumor-free survival curves (B) of 59 subjects with HCC classified into the L phenotype group (thin;  $n = 37$ ) and the H phenotype group (thick;  $n = 22$ ) after curative resection ( $P < .001$ ).

**Clinicopathologic analyses of gene-expression phenotypes.** To determine differences between L and H gene-expression phenotypes, clinicopathologic analyses were performed on 59 test cases (Table I). Statistical differences were found in tumor size ( $P = .023$ ), histologic differentiation ( $P = .002$ ), and pre-operative tumor makers, including either AFP ( $P = .002$ ) or PIVKA-II ( $P = .045$ ). In total, there were differences of overall survival ( $P < .001$ ) and tumor-free survival ( $P < .001$ ) between L phenotypes (37 cases) and H phenotypes (22 cases; Fig 2). Statistical risk factors for HCC recurrence were determined by univariate analyses; the gene-expression phenotype ( $P < .001$ ) as well as the clinicopathologic vascular invasion ( $P < .001$ ), number of neoplasms ( $P = .036$ ), size of neoplasm ( $P = .038$ ), histologic differentiation ( $P =$

Table II. Univariate risk factors of HCC recurrence

| Variables of primary HCC    | Number of cases | Recurrence rate/year* | P value* |
|-----------------------------|-----------------|-----------------------|----------|
| Gene-expression phenotype   |                 |                       | <.001    |
| L phenotype                 | 37              | 0.259                 |          |
| H phenotype                 | 22              | 0.762                 |          |
| Vascular invasion           |                 |                       | <.001    |
| V0 (none)                   | 30              | 0.407                 |          |
| V1 (microvascular invasion) | 14              | 0.425                 |          |
| V2 (macrovascular invasion) | 15              | 0.885                 |          |
| Number of neoplasms         |                 |                       | .036     |
| <3                          | 50              | 0.414                 |          |
| >3                          | 9               | 0.8                   |          |
| Size of neoplasm            |                 |                       | .038     |
| <4 cm                       | 31              | 0.293                 |          |
| >4 cm                       | 28              | 0.74                  |          |
| Histologic differentiation  |                 |                       | .027     |
| Well                        | 13              | 0                     |          |
| Moderate/poor               | 46              | 0.598                 |          |
| PIVKA-II                    |                 |                       | .030     |
| <300 mAU/mL                 | 33              | 0.272                 |          |
| >300 mAU/mL                 | 26              | 0.721                 |          |

\*Recurrence rates and  $P$  values were determined using the Kaplan-Meier method and the log-rank test.

.027), and level of PIVKA-II ( $P = .030$ ) (Table II). Multivariate analysis for recurrence indicated L-H gene-expression phenotypes ( $P = .031$ ) and level of PIVKA-II ( $P = .048$ ) as independent (risk) factors but not macrovascular invasion ( $P = .124$ ) or microvascular invasion per se ( $P = .274$ ; Table III).

**Validation analyses of gene-expression phenotypes.** The phenotypes of vascular invasion of patients with HCC according to the pattern of gene expression were identified with 132 and 172 probe sets using JT tests (Fig 1, A, Supplementary Table I) and Wilcoxon rank sum tests (Fig 1, B, Supplementary Table II). Among these probe sets, 93 genes were identified commonly by both JT and Wilcoxon tests (see Supplementary Table III in the online version at doi: 10.1016/j.surg.2007.09.037). To validate the phenotypes of gene expression, an additional 129 HCC cases composed of V0 ( $n = 67$ ), V1 ( $n = 33$ ), and V2 ( $n = 29$ ) were analyzed for hierarchical clustering using the 93 genes identified by 2 test analyses. As shown in Fig 3, A, no cluster was evident when V1 cases were analyzed. Two dendrograms by the hierarchical clustering provided similar assignment results for 33 V1 cases that were separated into L phenotypes (18 cases) and H

**Table III.** Results of Cox multivariate analysis on risk factors of HCC recurrence

| Variables of primary HCC   | Coefficient | Odds ratio | 95% confidence interval | P value |
|----------------------------|-------------|------------|-------------------------|---------|
| Gene-expression phenotype  | 1.685       | 5.390      | 1.167–24.905            | .031    |
| Macrovascular invasion     | 1.033       | 2.809      | 0.755–10.455            | .124    |
| Microvascular invasion     | 0.822       | 2.274      | 0.521–9.919             | .274    |
| Number of neoplasms        | 0.436       | 1.546      | 0.436–5.483             | .500    |
| Size of neoplasm           | 0.390       | 1.477      | 0.519–4.201             | .465    |
| Histologic differentiation | 1.238       | 3.450      | 0.400–29.777            | .260    |
| Serum level of PIVKA-II    | 1.009       | 2.744      | 1.007–7.476             | .048    |

phenotypes (15 cases). Indeed, tumor recurrence in V1 subjects demonstrated significant differences between 2 gene-expression phenotypes. As shown in Fig 3, *B*, tumor-free survivals of L phenotypes were better compared with those of H phenotypes within the V1 cases ( $P = .039$ ). Gene profiling revealed the microvascular invasiveness consisted of a classable mixture of L and H phenotypes, substantially affecting prognoses.

Among the 93 commonly identified genes, 28 genes were upregulated in the H phenotype (Table IV). Several cytokinesis-related genes were found, including aurora kinase B (AURKB), translocated promoter region, centromere protein I (CENPI), chromobox homolog 1 (CBX1), stathmin 1/oncoprotein 18 (STMN1), nuclear transcription factor Y alpha (NFYA), citron/rho-interacting, serine/threonine kinase 21 (CIT), cyclin F (CCNF), importin 9 (IPO9), metastasis associated 1 family member 3 (MTA3), exportin 1 (XPO1), and minichromosome maintenance 8 (MCM8). Interestingly, STMN1 is a direct substrate of AURKB,<sup>13</sup> and other molecules such as CENPI, CBX1, and CIT are regulated indirectly by AURKB.<sup>14,16</sup> According to biomolecular interaction network analyses using these cytokinesis-related genes, the AURKB pathway seems to be activated in H phenotypes with HCC vascular invasion (Fig 4, *A*).

**AURKB protein overexpressed in HCC tissues in association with gene-expression phenotypes.** To validate the expression of AURKB detected by microarrays, immunohistochemical studies were performed on 89 HCC cases composed of 58 L-phenotypes and 31 H-phenotypes using anti-AURKB antibodies (ab2254; Novus Biologicals Inc.) at 1:50 dilutions with PBS containing 1% bovine serum albumin (Sigma), followed by reactions in an automated immunostainer Ventana XT System. Strong, diffuse nuclear staining in AURKB was observed only in HCC tumor tissues but not in the adjacent normal tissues of the liver (Fig 4, *B*). AURKB protein was detected in 32 of 89 cases

(36%). The microarray intensity of the AURKB gene was greater in the 32 cases compared with the remaining 57 cases ( $FC = 2.4$ ;  $P = .001$ ). The results of immunohistochemical analyses confirmed microarray findings at the level of protein expression. The overexpression of AURKB protein was recognized in 24 of 31 H-phenotypes but only in 8 of 58 L-phenotypes in total ( $P < .001$ ). Within 22 V1 cases, 8 of 12 H-phenotypes but only 1 of 10 L-phenotypes were positive for AURKB protein ( $P = .002$ ).

## DISCUSSION

Vascular invasiveness is a major factor that reflects the biologically aggressive phenotype in HCC.<sup>4,8</sup> Because various molecules seem to regulate the macrovascular invasiveness in HCC,<sup>17-21</sup> it may be possible to determinate biologic significances of microvascular invasion (V1) and to distinguish microvascular from macrovascular invasion (V2). In this study, we analyzed genome-wide gene expression using microarray profiling (Fig 1). As shown by hierarchical clustering, V0 and V2 cases were clearly divided into 2 major clusters (L and H) based on JT or Wilcoxon analyses; however, the V1 cases with microvascular invasion did not form a cluster (Fig 1, *A* and *B*). It is noteworthy that both hierarchical clustering analyses provided exactly the same assignment results for V1 subjects. In total, V0, V1, and V2 cases were classified into 2 dendrograms, L (37 cases) and H (22 cases) phenotypes. The prognosis was different between L and H phenotypes in overall survival ( $P < .001$ ) and tumor-free survival ( $P < .001$ ; Fig 2). Furthermore, a multivariate analysis for the tumor recurrence indicated that the L-H gene phenotypes of gene expression ( $P = .031$ ) were an independent (risk) factor (Table III) but not the V0-V1-V2 clinicopathologic vascular invasion per se, which was identified only by univariate analyses (Table II).

Histologic V1 cases may consist of 2 components, namely, L and H phenotypes. Using gene-

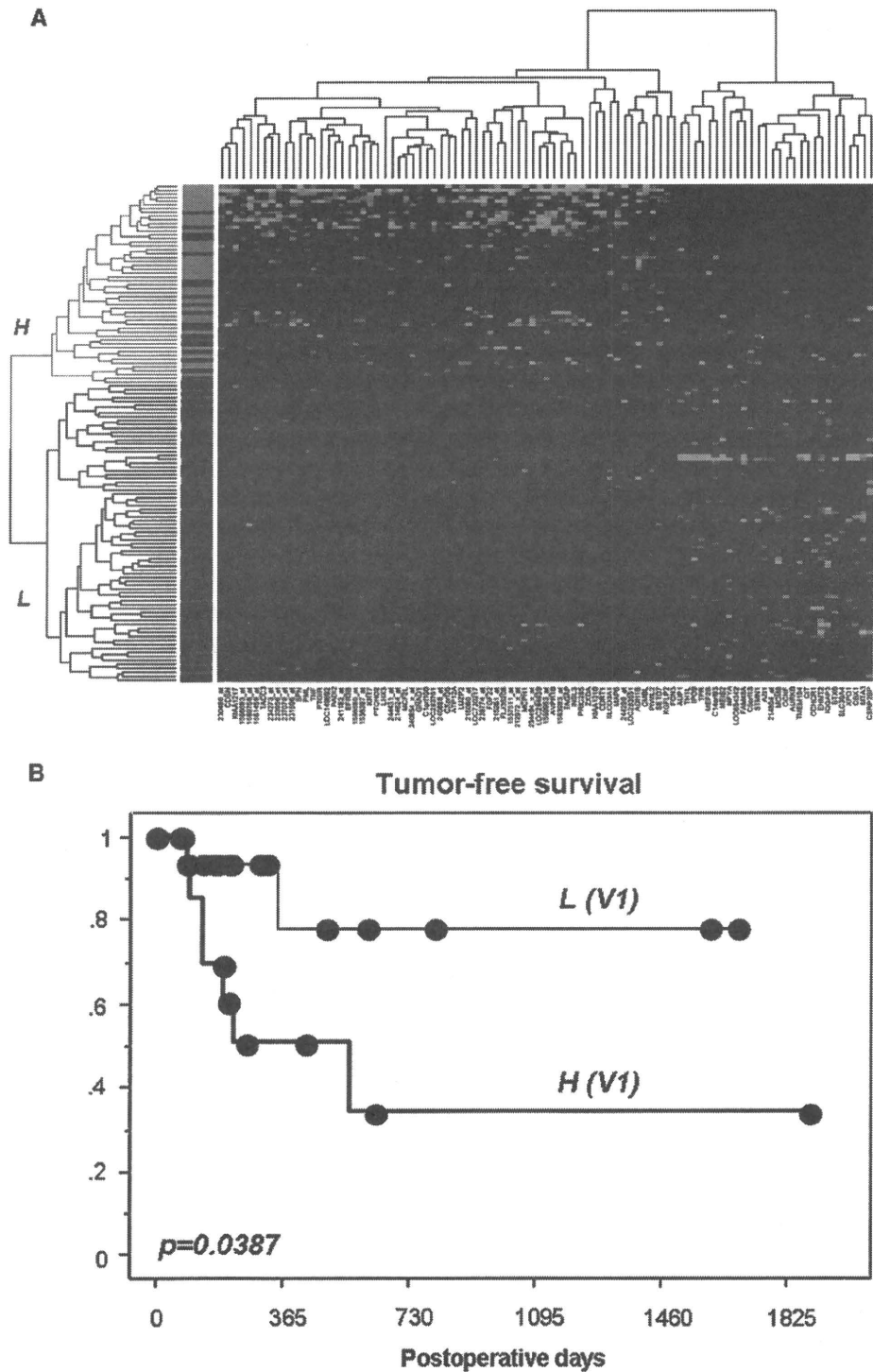


**Fig 3.** Validation analyses of gene-expression phenotypes using the 93 probe sets in additional 129 cases with HCC composed of 67 V0 cases (black bar), 33 V1 cases (blue bar), and 29 V2 cases (orange bar). (A) Hierarchical clustering of gene-expression profiles. Dendrograms show the classification determined by hierarchical clustering analyses: less (L) and highly (H) invasive phenotypes. Red and green colors indicate relative overexpression and underexpression, respectively. Two dendrograms by the hierarchical clustering provided similar assignment results for the 33 V1 cases that separated into the L phenotype (18 cases) and H phenotype (15 cases). (B) Tumor-free survival curves of 33 V1 cases with HCC classified into the L phenotype group (thin) and the H phenotype group (thick) after curative resection ( $P = .039$ ).



**Table IV.** Gene lists commonly upregulated in the H phenotype by both JT and Wilcoxon rank sum tests

| Probe set ID | Gene symbol | Gene title  | JT       |       | Wilcoxon |       | Fold change |
|--------------|-------------|---|----------|-------|----------|-------|-------------|
|              |             |   | P value  | FDR   | P value  | FDR   |             |
| 209464_at    | AURKB       | Aurora kinase B   | 1.07E-04 | 0.050 | 3.55E-05 | 0.035 | 2.36        |
| 214742_at    | AZI1        | 5-azacytidine induced 1                                   | 1.20E-04 | 0.050 | 7.52E-05 | 0.043 | 1.46        |
| 242133_s_at  | LOC654342   | Similar to lymphocyte-specific protein 1                  | 7.96E-05 | 0.049 | 1.21E-04 | 0.048 | 2.58        |
| 201730_s_at  | TPR         | Translocated promoter region (to activated MET oncogene)  | 7.50E-05 | 0.049 | 5.88E-05 | 0.038 | 1.86        |
| 214804_at    | CENPI       | Centromere protein I                                      | 8.96E-05 | 0.049 | 9.56E-05 | 0.045 | 1.69        |
| 201518_at    | CBX1        | Chromobox homolog 1 (HP1 beta homolog <i>Drosophila</i> ) | 9.51E-05 | 0.049 | 1.36E-04 | 0.049 | 1.68        |
| 42361_g_at   | CCHCR1      | Coiled-coil alpha-helical rod protein 1                   | 8.45E-05 | 0.049 | 1.40E-06 | 0.010 | 1.57        |
| 217714_x_at  | STMN1       | Stathmin 1/oncoprotein 18                                 | 7.73E-05 | 0.049 | 6.65E-05 | 0.040 | 1.52        |
| 220525_s_at  | AUP1        | Ancient ubiquitous protein 1                              | 8.45E-05 | 0.049 | 1.36E-04 | 0.049 | 1.33        |
| 229538_s_at  | IQGAP3      | IQ motif containing GTPase activating protein 3           | 6.27E-05 | 0.048 | 1.52E-04 | 0.049 | 2.24        |
| 215720_s_at  | NFYA        | Nuclear transcription factor Y, alpha                     | 5.39E-05 | 0.046 | 1.83E-05 | 0.029 | 1.41        |
| 225865_x_at  | TH1L        | TH1-like ( <i>Drosophila</i> )                            | 5.23E-05 | 0.045 | 1.04E-05 | 0.020 | 1.54        |
| 219215_s_at  | SLC39A4     | Solute carrier family 39 (zinc transporter), member 4     | 4.09E-05 | 0.042 | 3.55E-05 | 0.035 | 4.42        |
| 207480_s_at  | MEIS2       | Meis homeobox 2   | 4.09E-05 | 0.042 | 3.11E-05 | 0.035 | 2.28        |
| 212801_at    | CIT         | Citron (rho-interacting, serine/threonine kinase 21)      | 2.19E-05 | 0.042 | 1.95E-06 | 0.010 | 2.26        |
| 212621_at    | KIAA0286    | KIAA0286 protein  | 4.09E-05 | 0.042 | 5.19E-05 | 0.038 | 1.99        |
| 226330_s_at  | FAM48A      | Family with sequence similarity 48, member A              | 2.82E-05 | 0.042 | 2.39E-05 | 0.034 | 1.83        |
| 204826_at    | CCNF        | Cyclin F  | 3.40E-05 | 0.042 | 2.32E-07 | 0.010 | 1.72        |
| 217885_at    | IPO9        | Importin 9  | 3.40E-05 | 0.042 | 5.88E-05 | 0.038 | 1.64        |
| 223311_s_at  | MTA3        | Metastasis associated 1 family, member 3                  | 2.65E-05 | 0.042 | 9.56E-05 | 0.045 | 1.61        |
| 228544_s_at  | CSRP2BP     | CSRP2 binding protein                                     | 3.40E-05 | 0.042 | 1.49E-04 | 0.049 | 1.57        |
| 208775_at    | XPO1        | Exportin 1 (CRM1 homolog, yeast)                          | 3.73E-05 | 0.042 | 1.52E-04 | 0.049 | 1.44        |
| 219009_at    | C14orf93    | Chromosome 14 open reading frame 93                       | 3.73E-05 | 0.042 | 8.05E-06 | 0.018 | 1.43        |
| 230424_at    | C5orf13     | Chromosome 5 open reading frame 13                        | 1.31E-05 | 0.034 | 5.82E-06 | 0.016 | 2.56        |
| 202326_at    | EHMT2       | Euchromatic histone-lysine N-methyltransferase 2          | 7.73E-06 | 0.034 | 5.88E-05 | 0.038 | 1.80        |
| 214441_at    | STX6        | Syntaxin 6  | 8.82E-06 | 0.034 | 2.73E-05 | 0.034 | 1.24        |
| 224320_s_at  | MCM8        | Minichromosome maintenance complex component 8            | 2.26E-06 | 0.034 | 4.30E-06 | 0.016 | 2.34        |
| 1553978_at   | MEF2B       | Myocyte enhancer factor 2B                                | 6.32E-06 | 0.034 | 1.65E-06 | 0.010 | 1.49        |

expression patterns identified by both JT and Wilcoxon rank sum tests, additional analyses of hierarchical clustering on different cases validated that the other V1 subjects separated into 2 expression phenotypes as expected (Fig 3, A). Although 5 V0 cases were located in the H area, the number was too small to show a statistical difference in survival compared with the other V0 cases. It is noteworthy that there were differences in tumor recurrence in V1 subjects between the 2 gene-expression phenotypes of L and H (Fig 3, B). These novel findings may question whether operative resection or liver transplantation is the best therapeutic option for some of these HCCs.<sup>22</sup> Gross macrovascular invasion is a well-known independent predictor of tumor

recurrence after liver transplantations<sup>23,24</sup>; however, the importance of microvascular invasion remains controversial. Several recent reports suggested that microvascular invasion did not seem to be an independent factor for survival.<sup>25,26</sup> Furthermore, the Barcelona Group proposed salvage transplantation even in the absence of proven residual disease in subjects after hepatic resection when pathologic microvascular invasion was noted.<sup>27</sup> According to their results for 5 transplanted cases, 1 subject presented extrahepatic dissemination early after the transplantation and died 4 months later. Together with our microarray profiling, the H gene phenotype in a patient with microvascular invasion could not be overcome by liver transplantation.

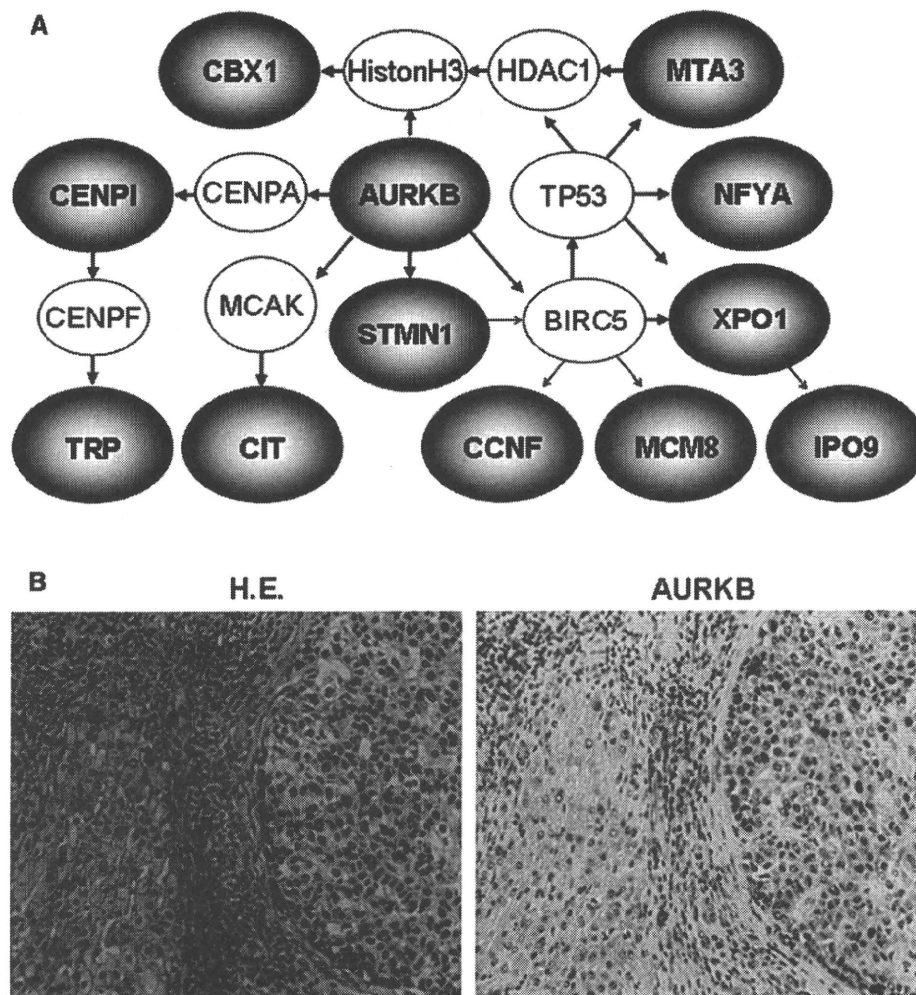


**Fig 4.** Network pathway and immunodetection in HCC. (A) Biomolecular interaction network analyses of commonly up-regulated genes by both JT and Wilcoxon rank sum tests of complementary DNA (cDNA) microarray data. The AURKB related pathway is composed of 12 upregulated genes (red circles). Bold arrows indicate direct protein-protein interactions, and thin arrows indicate indirect interactions. (B) Immunohistochemical analyses of AURKB in HCC tissues (magnification;  $\times 100$ ). AURKB protein in cancer cell nuclei, but not in adjacent noncancerous hepatocytes (left panel). Hematoxylin-eosin staining (H.E.; right panel).

Biomolecular network interaction analyses on criteria of H phenotypes revealed that vascular invasion may be associated with the upregulation of the AURKB-related pathway (Fig 4, A) and protein overexpression of AURKB was confirmed by immunohistochemistry (Fig 4, B). AURKB is a chromosomal passenger serine/threonine protein kinase that regulates accurate chromosomal segregation, cytokinesis, and protein localization to the centromere and kinetochore, corrects microtubule-kinetochore attachments, and regulates the mitotic checkpoint.<sup>28</sup> Our previous studies on HCC recurrences revealed that AURKB expression is associated closely with genetic instability in HCC.<sup>11</sup> Pathway genes such as CCNF and

MCM8 also relate to genetic instability.<sup>29,30</sup> More importantly, AURKBs have received recently increasing attention as eligible targets in molecular cancer therapies.<sup>31,32</sup> An AURKB-targeted therapy might be a promising, neoadjuvant approach for occult vascular invasion in HCC.

In conclusion, gene-expression profiling revealed that neoplasms containing microvascular invasion are composed of classable mixtures of less invasive and highly invasive phenotypes. Randomized trials as well as longer observation times are required to prove critical impacts of oncologic profiling. Our findings suggest that attention should be directed at the heterogeneity of HCC with microvascular invasion when considering

hepatic resection and liver transplantation. There should be additional analyses on specific gene-expression profiles that associate with an increased risk of recurrence and poor survival.

#### REFERENCES

- Ince N, Wands JR. The increasing incidence of hepatocellular carcinoma. *N Engl J Med* 1999;340:798-9.
- Arii S, Yamaoka Y, Futagawa S, Inoue K, Kobayashi K, Kojiro M, et al. Results of surgical and nonsurgical treatment for small-sized hepatocellular carcinomas: a retrospective and nationwide survey in Japan. The Liver Cancer Study Group of Japan. *Hepatology* 2000;32:1224-9.
- Tanaka S, Noguchi N, Ochiai T, Kudo A, Nakamura N, Ito K, et al. Outcomes and recurrence of initially resection of hepatocellular carcinoma meeting Milan criteria: rationale for partial hepatectomy as first strategy. *J Am Coll Surg* 2007;204:1-6.
- Kumada T, Nakano S, Takeda I, Sugiyama K, Osada T, Kiriyama S, et al. Patterns of recurrence after initial treatment in patients with small hepatocellular carcinoma. *Hepatology* 1997;25:87-92.
- Izumi R, Shimizu K, Ii T, Yagi M, Matsui O, Nonomura A, et al. Prognostic factors of hepatocellular carcinoma in patients undergoing hepatic resection. *Gastroenterology* 1994;106:720-7.
- Shimada M, Takenaka K, Gion T, Fujiwara Y, Kajiyama K, Maeda T, et al. Prognosis of recurrent hepatocellular carcinoma: a 10-year surgical experience in Japan. *Gastroenterology* 1996;111:720-6.
- Poon RT, Fan ST, Lo CM, Liu CL, Wong J. Intrahepatic recurrence after curative resection of hepatocellular carcinoma: long-term results of treatment and prognostic factors. *Ann Surg* 1999;229:216-22.
- Ohkubo T, Yamamoto J, Sugawara Y, Shimada K, Yamasaki S, Makuuchi M, et al. Surgical results for hepatocellular carcinoma with macroscopic portal vein tumor thrombosis. *J Am Coll Surg* 2000;191:657-60.
- Iizuka N, Oka M, Yamada-Okabe H, Nishida M, Maeda Y, Mori N, et al. Oligonucleotide microarray for prediction of early intrahepatic recurrence of hepatocellular carcinoma after curative resection. *Lancet* 2003;361:923-9.
- Thomas MB, Abbruzzese JL. Opportunities for targeted therapies in hepatocellular carcinoma. *J Clin Oncol* 2005; 23:8093-108.
- Tanaka S, Arii S, Yasen M, Mogushi K, Su NT, Zhao C, et al. Aurora kinase B is a predictive factor for aggressive recurrence of hepatocellular carcinoma after curative hepatectomy. *Br J Surg* 2008;95:611-9.
- Dahlquist KD, Salomonis N, Vranizan K, Lawlor SC, Conklin BR. GenMAPP, a new tool for viewing and analyzing microarray data on biological pathways. *Nat Genet* 2002; 31:19-20.
- Gadea BB, Ruderman JV. Aurora B is required for mitotic chromatin-induced phosphorylation of Op18/Stathmin. *Proc Natl Acad Sci U S A* 2006;103:4493-8.
- Liu ST, Rattner JB, Jablonski SA, Yen TJ. Mapping the assembly pathways that specify formation of the trilaminar kinetochore plates in human cells. *J Cell Biol* 2006;175:41-53.
- Ayoub N, Jeyasekharan AD, Bernal JA, Venkitaraman AR. HP1-beta mobilization promotes chromatin changes that initiate the DNA damage response. *Nature* 2008;453:682-6.
- Chalamalasetty RB, Hümmer S, Nigg EA, Silljé HH. Influence of human Ect2 depletion and overexpression on cleavage furrow formation and abscission. *J Cell Sci* 2006;119:3008-19.
- Arii S, Mise M, Harada T, Furutani M, Ishigami S, Niwano M, et al. Overexpression of matrix metalloproteinase 9 gene in hepatocellular carcinoma with invasive potential. *Hepatology* 1996;24:316-22.
- Tanaka S, Mori M, Sakamoto Y, Makuuchi M, Sugimachi K, Wands JR. Biologic significance of angiopoietin-2 expression in human hepatocellular carcinoma. *J Clin Invest* 1999;103:341-5.
- Liu SH, Lin CY, Peng SY, Jeng YM, Pan HW, Lai PL, et al. Down-regulation of annexin A10 in hepatocellular carcinoma is associated with vascular invasion, early recurrence, and poor prognosis in synergy with p53 mutation. *Am J Pathol* 2002;160:1831-7.
- Ho MC, Lin JJ, Chen CN, Chen CC, Lee H, Yang CY, et al. A gene expression profile for vascular invasion can predict the recurrence after resection of hepatocellular carcinoma: a microarray approach. *Ann Surg Oncol* 2006;13:1474-84.
- Kaposi-Novak P, Lee JS, Gomez-Quiroz L, Coulouarn C, Factor VM, Thorgeirsson SS. Met-regulated expression signature defines a subset of human hepatocellular carcinomas with poor prognosis and aggressive phenotype. *J Clin Invest* 2006;116:1582-95.
- Nakashima Y, Nakashima O, Tanaka M, Okuda K, Nakashima M, Kojiro M. Portal vein invasion and intrahepatic micrometastasis in small hepatocellular carcinoma by gross type. *Hepato Res* 2003;26:142-7.
- Mazzafarro V, Regalia E, Doci R, Andreola S, Pulvirenti A, Bozzetti F, et al. Liver transplantation for the treatment of small hepatocellular carcinoma in patients with cirrhosis. *N Engl J Med* 1996;334:693-9.
- Todo S, Furukawa H. Japanese Study Group on Organ Transplantation. Living donor liver transplantation for adult patients with hepatocellular carcinoma: experience in Japan. *Ann Surg* 2004;240:451-9.
- Shetty K, Timmins K, Brensinger C, Furth EE, Rattan S, Sun W, et al. Liver transplantation for hepatocellular carcinoma validation of present selection criteria in predicting outcome. *Liver Transpl* 2004;10:911-8.
- Shah SA, Tan JC, McGilvray ID, Cattral MS, Levy GA, Greig PD, et al. Does microvascular invasion affect outcomes after liver transplantation for HCC? A histopathological analysis of 155 consecutive explants. *J Gastrointest Surg* 2007;11:464-71.
- Sala M, Fuster J, Llovet JM, Navasa M, Solé M, Varela M, et al. High pathological risk of recurrence after surgical resection for hepatocellular carcinoma: an indication for salvage liver transplantation. *Liver Transpl* 2004;10:1294-300.
- Vader G, Medema RH, Lens SM. The chromosomal passenger complex: guiding Aurora-B through mitosis. *J Cell Biol* 2006;173:833-7.
- Takahashi K, Yamada H, Yanagida M. Fission yeast minichromosome loss mutants mis cause lethal aneuploidy and replication abnormality. *Mol Biol Cell* 1994;5:1145-58.
- Rajagopalan H, Jallepalli PV, Rago C, Velculescu VE, Kinzler KW, Vogelstein B, et al. Inactivation of hCDC4 can cause chromosomal instability. *Nature* 2004;428:77-81.
- Girdler F, Gascoigne KE, Evers PA, Hartmuth S, Crafter C, Foote KM, et al. Validating Aurora B as an anti-cancer drug target. *J Cell Sci* 2006;119:3664-75.
- Aihara A, Tanaka S, Yasen M, Matsumura S, Mitsunori Y, Murakata A, et al. The selective Aurora B kinase inhibitor AZD1152 as a novel treatment for hepatocellular carcinoma. *J Hepatol*. In press.

## Current status of molecularly targeted therapy for hepatocellular carcinoma: basic science

Shinji Tanaka · Shigeki Arii

Received: 31 March 2010 / Published online: 27 May 2010  
© Japan Society of Clinical Oncology 2010

**Abstract** Conventional systemic chemotherapy has been developed with so-called anti-cancer agents, essentially screened for cytotoxicity to cultured cancer cells. However, in patients with hepatocellular carcinoma (HCC), the role of chemotherapy is quite limited because most anti-cancer agents are ineffective and relatively toxic to HCC patients with chronic liver diseases. On the other hand, accumulated understanding of the molecular mechanisms regulating cancer progression has led to novel development of molecularly targeted therapies with cytostatic agents. Recently, a phase III clinical trial revealed a multi-kinase inhibitor, Sorafenib, as the first agent leading to improved overall survival of patients with advanced HCC. A new era of HCC treatment has arrived, based on identification of deranged signaling pathways of cancer cells or their microenvironment. This review summarizes the molecular hallmarks of HCC with a focus on angiogenesis, growth signals, and mitotic stress, and a novel concept “synthetic lethality” for the targeted therapy strategy.

**Keywords** Angiogenesis · Growth signals · Mitotic stress · Aurora · Synthetic lethality

### Introduction

A decade ago, Hanahan and Weinberg [1] proposed six hallmarks of cancer that collectively promote survival and

proliferation in foreign environments (Fig. 1). The hallmarks consist of self-sufficiency in growth signals, insensitivity to anti-growth signals, limitless replicative potential, evasion of apoptosis, tissue invasion and metastasis, and sustained angiogenesis. Subsequently, additional hallmarks, “evading immune surveillance” and five “stress phenotypes”, were expanded by Kroemer et al. [2] and Elledge et al. [3], respectively. A total of twelve hallmarks have been suggested as oncogene and non-oncogene addictions of cancer cells [3, 4] (Fig. 1). More important, these addictive hallmarks might be inextricably linked to molecular targets for cancer treatment, as the Achilles “heals” of cancer cells [5]. Numerous studies on molecular abnormalities in hepatocellular carcinoma (HCC) progression have revealed the crucial roles of such hallmarks in the pathogenesis [6]. Among these, this review focuses on three hallmarks of HCC; “sustained angiogenesis”, “self-sufficiency in growth signals”, and “mitotic stress”, in respect of substantially and/or potentially targeted therapy for HCC [7, 8].

### Sustained angiogenesis

In-vivo tumor progression requires the supply of oxygen and nutrition by the vasculature [9]. HCC is a typical angiogenic tumor, because dramatic alteration in the arterial vascularity is usually recognized in moderately-to-poorly differentiated types of HCC, leading to acquisition of the potential for vascular invasiveness and metastasis [10]. Blood vessels consist of endothelial cells and the externally shielding pericytes. Vascular endothelial growth factor (VEGF) is one of the potent factors stimulating the growth and migration of the endothelial cells [11]. We first found a close relationship between VEGF expression and

S. Tanaka (✉) · S. Arii  
Department of Hepato-Biliary-Pancreatic Surgery,  
Graduate School of Medicine, Tokyo Medical  
and Dental University, 1-5-45 Yushima, Bunkyo-ku,  
Tokyo 113-8519, Japan  
e-mail: shinji.msrg@tmd.ac.jp



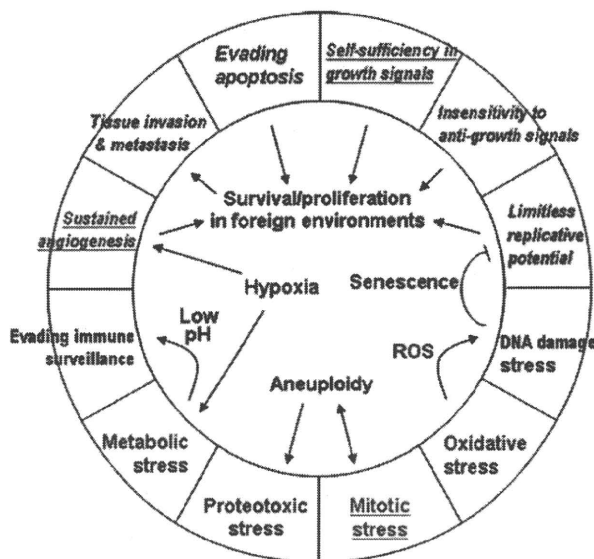


**Fig. 1** Twelve hallmarks of cancer [3]. The top six hallmarks (*italics*) were originally proposed by Hanahan and Weinberg in 2000 [1]. The additional hallmark “evading immune surveillance” (*left*) and five “stress phenotypes” (*bottom*), were expanded by Kroemer et al. [2] and Elledge et al. [3], respectively. Three hallmarks “sustained angiogenesis”, “self-sufficiency in growth signals”, and “mitotic stress” are the focus of this review (*underlined*)

HCC progression in a clinical specimen [12]. It is of interest that the receptors VEGFR1/Flt-1 and VEGFR2/KDR/Flk-1 were recognized not only on vascular endothelial cells but also on human HCC cells [13]. According to basic studies on murine tumor models, VEGFR1-expressing hematopoietic cells might play critical roles in formation of the premetastatic niche [14, 15]. Thus, the VEGF signaling might function not only as angiogenesis but also as cancer invasion and metastasis of HCC [16].

VEGF belongs to a family of structurally and functionally related growth factors including the platelet-derived growth factors (PDGFs) that broadly stimulate various phenotypes of cells including vascular pericytes, the other components of the vasculature [17]. In drosophila, PEGF/VEGF-like factors share a single receptor [17]. Additionally, dual inhibition of VEGF and PDGF signals was revealed to have more effective anti-angiogenic effects in in-vivo tumor models [18]. Another potent stimulator of the HCC angiogenesis is fibroblast growth factor (FGF) [12]. FGF is frequently associated with the inflammatory process, and overexpression has also been observed in chronic hepatitis and cirrhotic liver tissues [19]. Serous basic FGF levels were reported to correlate with clinico-pathological progression of HCC [20], and synergetic effects of FGF and VEGF might involve HCC angiogenesis [12].

Angiogenesis is orchestrated hierarchically by numerous factors acting on these cells and progenitor cells from the tissue and/or bone marrow. Together with the VEGF/VEGFR

system, a variety of angiogenic factors and their receptors have been nominated as therapeutic targets for HCC. Most of molecularly targeted agents can be broadly classified into two main categories: small-molecule kinase inhibitors and monoclonal antibodies [6]. Table 1 summarizes the main agents and the targeted molecules studied by clinical trials on the HCC patients. *Sorafenib* (Nexavar, BAY43-9006) is a unique multi-targeting small-molecule that inhibits the receptor tyrosine kinases (RTKs) of VEGFR2, VEGFR3, PDGFR-beta, c-kit, and Flt-3, and the Raf serine-threonine kinase in intracellular growth signal transduction [21] (Fig. 2). It is worthy of note that the recent phase III trial, Sorafenib HCC assessment randomized protocol (SHARP), revealed Sorafenib to be the first agent that improved overall survival of patients with advanced HCC [21]. Other multiple kinase inhibitors of VEGFRs and PDGFRs, *Sunitinib* (Sutent, SU11248), *Vatalanib* (PTK787/ZK222584), *Cediranib* (AZD2171), and *SU6668* (TSU-68), are now under active investigation in clinical trials. *Brivanib* (BMS-540215), another type of inhibitor of VEGFRs and FGFRs has been reported to be effective against Sorafenib-resistant HCC in the early phase of clinical trials. The other category of targeted agents includes monoclonal antibodies against VEGF-A and VEGFR-2, *Bevacizumab* (Avastin) and *Ramucirumab* (IMC-1121B), respectively. In addition to the single-agent trials, combination trials with cytotoxic drugs have also been conducted.

Furthermore, we previously isolated Angiopoietin-2 as another angiogenic pathway essential for HCC progression [22, 23]. The angiopoietin family contains specific ligands for Tie2 RTK on vascular endothelial cells [24]. Although Angiopoietin-1 makes the vasculature stable, Angiopoietin-2 destabilizes vessel formation. According to recent reports, Angiopoietin-1 stimulates only the homodimer of Tie2 tyrosine kinase whereas Angiopoietin-2 also induces hetero-dimerization of Tie2 with Tie1, leading to vascular instability [25]. Angiopoietin-2 might function as an initiator of angiogenic switch, promoting susceptibility to VEGF stimulation in the angiogenic progression [26]. It should be noted that a promising result of clinical trials on patients with renal cell carcinoma was recently reported in which an angiopoietin inhibitor AMG386 ( $2 \times \text{Con4[C]}$ ), a synthetic peptide with high affinity for Angiopoietin-2, fused to the constant region of human immunoglobulin G1 [27, 28]. AMG386 is being studied in combination with Sorafenib, and with cytotoxic chemotherapy, for a variety of other angiogenic tumors.

### Self-sufficiency in growth signals

In general, deregulation of RTKs occurs in HCC cells, and epidermal growth factor receptor (EGFR) and insulin-like

**Table 1** Molecularly targeted agents for hepatocellular carcinoma in clinical trials

| Agent                           | Classification          | Function   |
|---------------------------------|-------------------------|--|
| Sorafenib (Nexabar, BAY43-9006) | Small molecule compound | VEGFR2, VEGFR3, PDGFR- $\beta$ , Flt-3, c-KIT tyrosine kinase, Raf serine/threonine kinase inhibitor |
| Sunitinib (Sutent, SU11248)     | Small molecule compound | VEGFR1, VEGFR2, PDGFRs, Flt-3, c-KIT tyrosine kinase inhibitor                                       |
| Vatalanib (PTK787/ZK222584)     | Small molecule compound | VEGFR1, VEGFR2, VEGFR3, PDGFR- $\beta$ , c-KIT tyrosine kinase inhibitor                             |
| Cediranib (AZD2171)             | Small molecule compound | VEGFR1, VEGFR2, VEGFR3, PDGFRs, c-KIT tyrosine kinase inhibitor                                      |
| SU6688 (TSU-68)                 | Small molecule compound | VEGFR2, PDGF R- $\beta$ , FGFRs tyrosine kinase inhibitor  |
| Brivanib (BMS-540215)           | Small molecule compound | VEGFR1, VEGFR2, VEGFR3, FGFR1, FGFR2, FGFR3 tyrosine kinase inhibitor                                |
| Bevacizumab (Avastin)           | Monoclonal antibody     | VEGF-A-neutralization  |
| Ramcirumab (IMC-1121B)          | Monoclonal antibody     | VEGFR2-neutralization  |
| Gefitinib (Iressa, ZD1839)      | Small molecule compound | EGFR/ErbB1/Her1 tyrosine kinase inhibitor  |
| Erlotinib (Tarceva, OSI774)     | Small molecule compound | EGFR/ErbB1/Her1 tyrosine kinase inhibitor  |
| Lapatinib (Tykerb, GW572016)    | Small molecule compound | EGFR/ErbB1/Her1 and ErbB2/Her2/Neu tyrosine kinase inhibitor   |
| BMS-599626                      | Small molecule compound | EGFR/ErbB1/Her1 and ErbB2/Her2/Neu tyrosine kinase inhibitor   |
| Cetuximab (Erbixux)             | Monoclonal antibody     | EGFR/ErbB1/Her1-neutralization   |
| IMC-A12                         | Monoclonal antibody     | IGF-IR-neutralization  |
| AZD6244 (ARRY-142886)           | Small molecule compound | MEK serine/threonine tyrosine kinase inhibitor   |
| Everolimus (RAD001)             | Small molecule compound | mTOR serine/threonine kinase inhibitor   |
| Sirolimus (Rapamune)            | Small molecule compound | mTOR serine/threonine kinase inhibitor   |
| Bortezomib (Velcade)            | Small molecule compound | Proteasome inhibitor   |
| PXD101 (Belinostat)             | Small molecule compound | HDAC inhibitor   |
| PI-88                           | Small molecule compound | Heparanase inhibitor   |

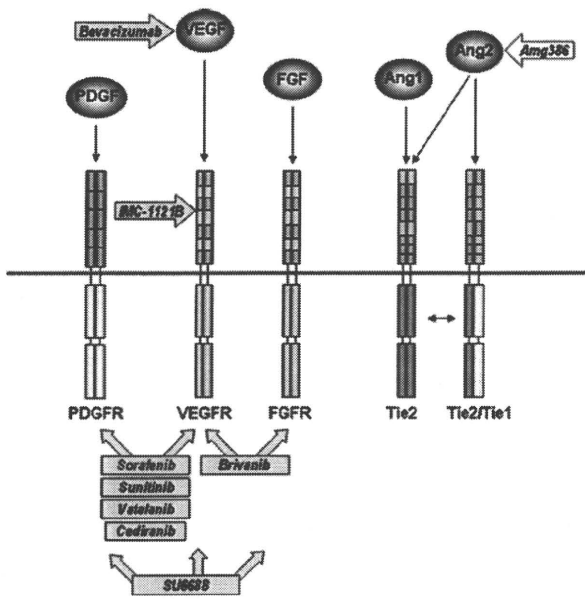


**Fig. 2** Molecular targets in angiogenesis with the growth factors and the receptors. Targeted agents are indicated by arrows

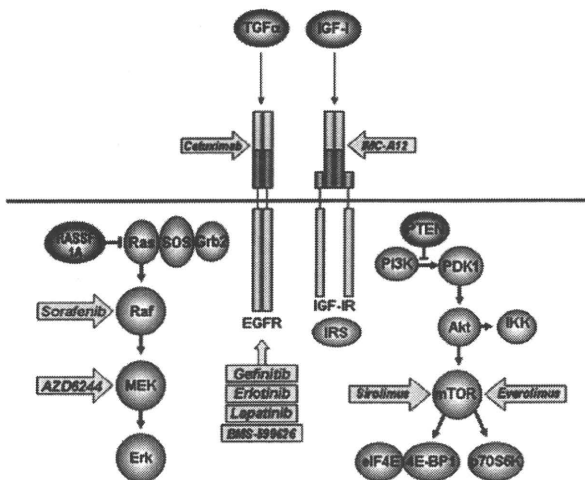


**Fig. 3** Molecular targets in HCC cells with the growth factors, receptors, and intracellular signaling. Targeted agents are indicated by arrows

growth factor-1 receptor (IGF-1R) are regarded as molecular targets for HCC treatment [6, 7] (Fig. 3). Clinical trials on HCC patients are ongoing with several tyrosine kinase inhibitors of EGFR—*Gefintinib* (Iressa, ZD1839), *Erlotinib* (Tarceva, OSI774), *Lapatinib* (Tykerb, GW572016), and *BMS-599626*. Monoclonal antibodies against EGFR (Cetuximab [Erbix]) and IGF-1R (IMC-A12) are also being evaluated for HCC in clinical trials.

The activated RTKs then stimulate several intracellular signal-transduction pathways including Ras/Raf/MEK/MAPK and PI3K/Akt/mTOR [29, 30] (Fig. 3). In a series

of specific phosphorylation events, an adaptor protein Grb2 stimulates SOS, leading to activation of oncogenic Ras, which is usually mutated in various malignancies. Despite the low incidence of Ras mutations in HCC, silencing with DNA methylation of the *RASSF1A* gene, a member of the RAS inhibitor family, was detected in human HCC [31]. The silencing of the RAS inhibitor might result in persistent activation of the downstream pathway during hepatocarcinogenesis. The activated form of Ras then stimulates Raf serine–threonine kinase that phosphorylates MEK kinases, and finally it activate the extracellular regulated kinase Erk of the MAPK family. The activated, Erk translocates to the nucleus where it acts as a regulator of gene expression of various proteins, including those of cell cycle progression, apoptosis resistance, and cellular motility [32]. As mentioned above, Raf kinase is one of the targets of the multi-kinase inhibitor *Sorafenib* [21]. Additionally, an MEK kinase inhibitor, *AZD6244* (ARRY-142886), has been evaluated for HCC in clinical trials.

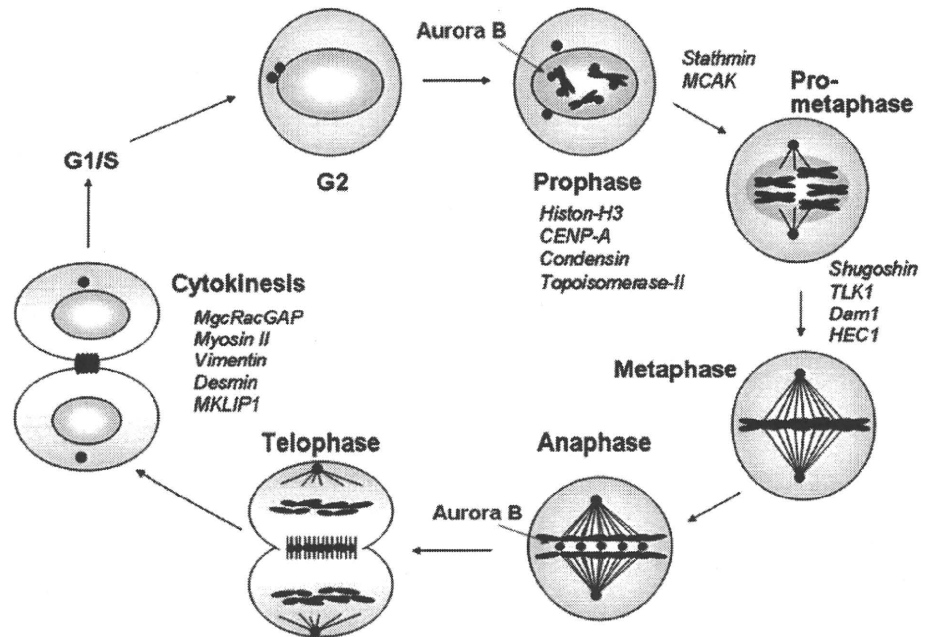
The PI3K/Akt/mTOR pathway has emerged as a contributor to hepatocarcinogenesis [33]. After association of PI3K with the intracellular domain of several RTKs or specific substrates such as IRS, PI3K phosphorylates PIP2 to generate PIP3 which transduces PDK, which activates a serine/threonine kinase Akt [32]. PIP3 is dephosphorylated by PTEN, a tumor suppressor which reverses this pathway. The activated Akt regulates multiple cellular target proteins such as the mammalian target of rapamycin (mTOR) [34]. The mTOR protein regulates the phosphorylation of p70 S6 serine–threonine kinase and the translational repressor protein 4E-BP1 [35]. As rapamycin-derivates, mTOR inhibitors temsirolimus (CCI-779) and *everolimus* (RAD001) are now under active investigation in clinical trials for patients with HCC.

**Mitotic stress**

Aneuploidy was noticed as one of the essential properties of cancer cells in the late nineteenth century. Recent studies clarified the increased rates of chromosome mis-segregation in mitosis, referred to as the chromosome instability (CIN) phenotype [36]. Cancer cells bearing mitotic abnormalities such as aneuploidy are likely to be more dependent on stress-support pathways for specific segregation of the chromosomes. In addition, the CIN phenotype could result from stresses placed on the mitotic apparatus because of the need to segregate abnormal chromosomes. Furthermore, mitotic stress might arise indirectly as a result of double-strand breaks and genomic instability after oncogene activation [3].

We have identified Aurora kinase B, a mitotic checkpoint kinase, as a unique molecule for predicting the lethal

**Fig. 4** Mitosis phase of the cell cycle. Localization of Aurora kinase B indicated by *arrows*. Main substrates of Aurora kinase B shown in *italics*



recurrence of HCC even after curative hepatectomy [37]. Array-CGH revealed the CIN phenotype of HCC was closely related to Aurora kinase B expression. Aurora kinase B is a chromosomal passenger protein that regulates accurate chromosomal segregation, cytokinesis, protein localization to the centromere and kinetochore, correct microtubule-kinetochore attachments, and regulation of the mitotic checkpoint (Fig. 4) [38]. Recent studies revealed that deregulation of Aurora kinase B directly caused CIN and aneuploidy, transforming epithelial cells [39].

More important, several small-molecule inhibitors of Aurora kinase have been developed as anti-cancer agents including ZM447439, VX-680, PHA-680632, AZD1152 and MLN 8054 [40]. In particular, Aurora kinase B may be a suitable anticancer target, because inhibition of Aurora kinase B rapidly results in catastrophic mitosis with senescence. In our studies to evaluate the effects of Aurora B inhibitor on human HCC, accumulation of polyploidy and apoptosis was observed in all of the cell lines after administration of the inhibitor [41]. We utilized a novel orthotopic xenograft model of liver tumors to explore tumor growth inhibition in situ. Aurora B inhibitor was administered to mice bearing human HCC orthotopic xenografts. Growth of liver tumors was found to be suppressed in all of the mice that had been treated with the Aurora B inhibitor. After drug administration, the mean liver tumor weight in those animals that had received Aurora B inhibitor was 10% of that in the control mice. Similar growth inhibition was observed in orthotopic xenografts using other HCC cell lines after administration of Aurora B inhibitor. In the orthotopic model, mice

survival was significantly enhanced by Aurora B inhibitor treatment in comparison with the control. All of the host tissues examined, including liver, bone marrow, kidney, intestine, and lung, were histologically normal in all experiments. Specific inhibition of Aurora kinases is a promising novel therapeutic approach for treatment of aggressive HCC [42].

#### “Synthetic lethality”, a novel strategy for molecularly targeted therapy

These mitotic kinases have been recognized as promising molecular targets—“Achilles’ heels” of various malignancies [3]. More recently, another mitotic kinase, PLK1, was identified as a specific molecule with synthetic lethal interactions with mutant Ras oncogenes in cancer cells [43] (Fig. 5a). “Synthetic lethality” is a concept from traditional genetic science on drosophila, first described by Dobzhansky in 1946 [44]. As shown in Fig. 5b, two genes (“A” and “B”) are said to be in a “synthetic lethal” relationship if a mutation in either gene alone is not lethal but mutations in both cause the death of the cell. This concept can be extended to situations in discovery of molecular targets [45]. In applying synthetic lethality to the discovery of agents targeting cancer cells, a screening program is designed to find a target gene that kills cells bearing a cancer-specific alteration, such as a mutated tumor-suppressor gene or an activated oncogene, but spares otherwise identical cells lacking the cancer-specific alteration. Such a gene can then be the target for developing an anticancer drug.



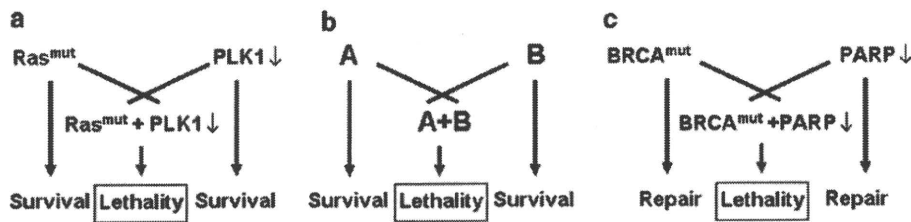


**Fig. 5** The concept of synthetic lethality. Synthetic lethal interactions were demonstrated with mutant Ras and PLK1 inhibition (a), the fundamental pattern of mutations A and B (b), and mutant BRCA and PARP inhibitor applied clinically (c)

In such screening programs for synthetic lethality to identify druggable targets that are unique to tumor cells but not normal cells [45], one successful and hopeful example has already been published as a phase I clinical trial of poly(ADP-ribose) polymerase 1 (PARP1) inhibitors in patients with hereditary breast and ovarian carcinomas with mutated BRCA1 and BRCA2 [46] (Fig. 5c). BRCA1 and BRCA2 are tumor-suppressor genes that are key participants in homologous recombination to repair DNA damage [47]. The enzyme activity of poly(ADP-ribose) polymerase 1 (PARP1) is required for base-excision repair, a DNA-damage repair pathway that recognizes and eliminates DNA bases damaged by oxidation in a process during each normal cell cycle. Normally, homologous recombination repairs these breaks, whereas in the case of absent BRCA1 or BRCA2, the cell dies without repair of the breaks. As predicted by the concept of synthetic lethality, small molecule inhibitors of PARP1 are toxic to cells deficient in BRCA1 or BRCA2, whereas cells in which BRCA1 or BRCA2 is restored are less sensitive to the inhibitors [48, 49]. According to these actual proofs with clinical benefits, the concept of synthetic lethality should be expanded not only to identification of novel druggable molecules but also to the rationale of addictions to oncogene and non-oncogene as the therapeutic targets. Further application of this synthetic lethal strategy must be actively engaged in developing a novel targeted therapy of HCC.

## Conclusion

HCC is one of the most common malignancies worldwide, and the incidence is still increasing [50]. The primary curative treatment for HCC is surgical resection, and there has been limited improvement in the availability of alternative treatments in the last decade [51]. Because there is an urgent need to develop novel treatments for HCC, the bench-to bedside translational approach should be implemented more intensely to elucidate the molecular mechanisms and therapeutic targets of advanced and/or recurrent HCC [52].

**Conflict of interest statement** No author has any conflict of interest.

## References

- Hanahan D, Weinberg RA (2000) The hallmarks of cancer. *Cell* 100(1):57–70
- Kroemer G, Pouyssegur J (2008) Tumor cell metabolism: cancer's Achilles' heel. *Cancer Cell* 13(6):472–482
- Luo J, Solimini NL, Elledge SJ (2009) Principles of cancer therapy: oncogene and non-oncogene addiction. *Cell* 136(5):823–837
- Weinstein IB (2002) Cancer. addiction to oncogenes—the Achilles heel of cancer. *Science* 297(5578):63–64
- Weinstein IB, Joe AK (2006) Mechanisms of disease: oncogene addiction—a rationale for molecular targeting in cancer therapy. *Nat Clin Pract Oncol* 3(8):448–457
- Tanaka S, Arii S (2009) Molecularly targeted therapy for hepatocellular carcinoma. *Cancer Sci* 100(1):1–8
- Llovet JM, Bruix J (2008) Molecular targeted therapies in hepatocellular carcinoma. *Hepatology* 48:1312–1327
- Yau T, Chan P, Epstein R et al (2009) Management of advanced hepatocellular carcinoma in the era of targeted therapy. *Liver Int* 29(1):10–17 Review
- Hanahan D, Folkman J (1996) Patterns and emerging mechanisms of the angiogenic switch during tumorigenesis. *Cell* 86:353–364
- Tanaka S, Arii S (2006) Current status of perspective of antiangiogenic therapy for cancer; hepatocellular carcinoma. *Int J Clin Oncol* 11:82–89
- Ferrara N (2002) VEGF and the quest for tumour angiogenesis factors. *Nat Rev Cancer* 2(10):795–803
- Mise M, Arii S, Higashitani H et al (1996) Clinical significance of vascular endothelial growth factor and basic fibroblast growth factor gene expression in liver tumor. *Hepatology* 23(3):455–464
- Schmitt M, Horbach A, Kubitz R et al (2004) Disruption of hepatocellular tight junctions by vascular endothelial growth factor (VEGF): a novel mechanism for tumor invasion. *J Hepatol* 41(2):274–283
- Kaplan RN, Riba RD, Zacharoulis S et al (2005) VEGFR1-positive haematopoietic bone marrow progenitors initiate the pre-metastatic niche. *Nature* 438(7069):820–827
- Hiratsuka S, Watanabe A, Aburatani H et al (2006) Tumour-mediated upregulation of chemoattractants and recruitment of myeloid cells predetermines lung metastasis. *Nat Cell Biol* 8(12):1369–1375
- Arii S (2004) Role of vascular endothelial growth factor on the invasive potential of hepatocellular carcinoma. *J Hepatol* 41(2):333–335

17. Andrae J, Gallini R, Betsholtz C (2008) Role of platelet-derived growth factors in physiology and medicine. *Genes Dev* 22(10):1276–1312
18. Kuhnert F, Tam BY, Sennino B et al (2008) Soluble receptor-mediated selective inhibition of VEGFR and PDGFRbeta signaling during physiologic and tumor angiogenesis. *Proc Natl Acad Sci USA* 105(29):10185–10190
19. Uematsu S, Higashi T, Nouse K et al (2005) Altered expression of vascular endothelial growth factor, fibroblast growth factor-2 and endostatin in patients with hepatocellular carcinoma. *J Gastroenterol Hepatol* 20(4):583–588
20. Poon RT, Ng IO, Lau C et al (2001) Correlation of serum basic fibroblast growth factor levels with clinicopathologic features and postoperative recurrence in hepatocellular carcinoma. *Am J Surg* 182:298–304
21. Llovet JM, Ricci S, Mazzaferro V et al (2008) Sorafenib in advanced hepatocellular carcinoma. *N Engl J Med* 359:378–390
22. Tanaka S, Mori M, Sakamoto Y et al (1999) Biologic significance of angiopoietin-2 expression in human hepatocellular carcinoma. *J Clin Invest* 103(3):341–345
23. Tanaka S, Wands JR, Arai S (2006) Induction of angiopoietin-2 gene expression by COX-2: A novel role for COX-2 inhibitors during hepatocarcinogenesis. *J Hepatol* 44(1):233–235
24. Tanaka S, Sugimachi K, Yamashita Yi et al (2002) Tie2 vascular endothelial receptor expression and function in hepatocellular carcinoma. *Hepatology* 35(4):861–867
25. Seegar TC, Eller B, Trzvetkova-Robev D et al (2010) Tie1–Tie2 interactions mediate functional differences between angiopoietin ligands. *Mol Cell* 37(5):643–655
26. Holash J, Maisonpierre PC, Compton D et al (1999) Vessel cooption, regression, and growth in tumors mediated by angiopoietins and VEGF. *Science* 284(5422):1994–1998
27. Oliner J, Min H, Leal J et al (2004) Suppression of angiogenesis and tumor growth by selective inhibition of angiopoietin-2. *Cancer Cell* 6(5):507–516
28. Herbst RS, Hong D, Chap L et al (2009) Safety, pharmacokinetics, and antitumor activity of AMG 386, a selective angiopoietin inhibitor, in adult patients with advanced solid tumors. *J Clin Oncol* 27(21):3557–3565
29. Pawson T (2004) Specificity in signal transduction: from phosphotyrosine–SH2 domain interactions to complex cellular systems. *Cell* 116:191–203
30. Tanaka S, Sugimachi K, Maehara S et al (2002) Oncogenic signal transduction and therapeutic strategy for hepatocellular carcinoma. *Surgery* 131:S142–S147
31. Schagdarsurengin U, Wilkens L, Steinemann D et al (2003) Frequent epigenetic inactivation of the RASSF1A gene in hepatocellular carcinoma. *Oncogene* 22:1866–1871
32. Farazi PA, DePinho RA (2006) Hepatocellular carcinoma pathogenesis: from genes to environment. *Nat Rev Cancer* 6:674–687
33. Luo J, Manning BD, Cantley LC (2003) Targeting the PI3K–Akt pathway in human cancer: rationale and promise. *Cancer Cell* 4:257–262
34. Chiang GG, Abraham RT (2007) Targeting the mTOR signaling network in cancer. *Trends Mol Med* 13:433–442
35. Foster KG, Fingar DC (2010) mTOR: conducting the cellular signaling symphony. *J Biol Chem*
36. Schwartzman JM, Sotillo R, Benezra R (2010) Mitotic chromosomal instability and cancer: mouse modelling of the human disease. *Nat Rev Cancer* 10(2):102–115
37. Tanaka S, Arai S, Yasen M et al (2008) Aurora kinase B is a predictive factor for the aggressive recurrence of hepatocellular carcinoma after curative hepatectomy. *Br J Surg* 95:611–619
38. Keen N, Taylor S (2004) Aurora-kinase inhibitors as anticancer agents. *Nat Rev Cancer* 4:927–936
39. Nguyen HG, Makitalo M, Yang D et al (2009) Deregulated Aurora-B induced tetraploidy promotes tumorigenesis. *FASEB J* 23(8):2741–2748
40. Harrington EA, Bebbington D, Moore J et al (2004) VX-680, a potent and selective small-molecule inhibitor of the Aurora kinases, suppresses tumor growth in vivo. *Nat Med* 10(3):262–267
41. Aihara A, Tanaka S, Yasen M et al (2010) The selective Aurora B kinase inhibitor AZD1152 as a novel treatment for hepatocellular carcinoma. *J Hepatol* 52(1):63–71
42. Tanaka S, Mogushi K, Yasen M et al (2010) Gene-expression phenotypes for vascular invasiveness of hepatocellular carcinomas. *Surgery* 147(3):405–414
43. Luo J, Emanuele MJ, Li D et al (2009) A genome-wide RNAi screen identifies multiple synthetic lethal interactions with the Ras oncogene. *Cell* 137(5):835–848
44. Dobzhansky T (1946) Genetics of natural populations. XIII. Recombination and variability in populations of *Drosophila pseudoobscura*. *Genetics* 31:269–290
45. Kaelin WG Jr (2005) The concept of synthetic lethality in the context of anticancer therapy. *Nat Rev Cancer* 5(9):689–698
46. Fong PC, Boss DS, Yap TA et al (2009) Inhibition of poly(ADP-ribose) polymerase in tumors from BRCA mutation carriers. *N Engl J Med* 361(2):123–134
47. Iglehart JD, Silver DP (2009) Synthetic lethality—a new direction in cancer-drug development. *N Engl J Med* 361(2):189–191
48. Bryant HE, Schultz N, Thomas HD et al (2005) Specific killing of BRCA2-deficient tumours with inhibitors of poly(ADP-ribose) polymerase. *Nature* 434(7035):913–917
49. Farmer H, McCabe N, Lord CJ et al (2005) Targeting the DNA repair defect in BRCA mutant cells as a therapeutic strategy. *Nature* 434(7035):917–921
50. Ince N, Wands JR (1999) The increasing incidence of hepatocellular carcinoma. *N Engl J Med* 340:798–799
51. Arai S, Yamaoka Y, Futagawa S et al (2000) Results of surgical and nonsurgical treatment for small-sized hepatocellular carcinomas: a retrospective and nationwide survey in Japan. The Liver Cancer Study Group of Japan. *Hepatology* 32:1224–1229
52. Tanaka S, Arai S (2010) Medical treatments: in association or alone, their role and their future perspectives: novel molecular-targeted therapy for hepatocellular carcinoma. *J Hepatobiliary Pancreat Surg*

## The selective Aurora B kinase inhibitor AZD1152 as a novel treatment for hepatocellular carcinoma

Arihiro Aihara, Shinji Tanaka\*, Mahmut Yassen, Satoshi Matsumura, Yusuke Mitsunori, Ayano Murakata, Norio Noguchi, Atsushi Kudo, Noriaki Nakamura, Koji Ito, Shigeki Arii

Department of Hepato-Biliary-Pancreatic Surgery, Graduate School of Medicine, Tokyo Medical and Dental University, 1-5-45 Yushima, Bunkyo-ku, Tokyo 113-8519, Japan

**Background & Aims:** We previously identified that high Aurora B expression was associated with hepatocellular carcinoma (HCC) recurrence due to tumor dissemination. In this preclinical study, a novel inhibitor of Aurora B kinase was evaluated as a treatment for human HCC.

**Methods:** AZD1152 is a selective inhibitor of Aurora B kinase. Twelve human HCC cell lines were analyzed for Aurora B kinase expression and the *in vitro* effects of AZD1152. The *in vivo* effects of AZD1152 were analyzed in a subcutaneous xenograft model and a novel orthotopic liver xenograft model.

**Results:** Aurora B kinase expression varied among the human HCC cell lines and was found to correlate with inhibition of cell proliferation, accumulation of 4N DNA, and the proportion of polyploid cells following administration of AZD1152-hydroxyquinazoline-pyrazol-anilide (AZD1152-HQPA). AZD1152-HQPA suppressed histone H3 phosphorylation and induced cell death in a dose-dependent manner. Growth of subcutaneous human HCC xenografts was inhibited by AZD1152 administration. In an orthotopic hepatoma model, treatment with AZD1152 significantly decelerated tumor growth and increased survival. Pharmacobiological analysis revealed that AZD1152 induced the rapid suppression of phosphohistone H3, followed by cellular apoptosis in the liver tumors but not in the normal tissues of the orthotopic models.

**Conclusions:** Our preclinical studies indicate that AZD1152 is a promising novel therapeutic approach for the treatment of HCC. © 2009 European Association for the Study of the Liver. Published by Elsevier B.V. All rights reserved.

### Introduction

Hepatocellular carcinoma (HCC) is one of the most common malignancies worldwide, accounting nearly for 1 million deaths per year

**Keywords:** Hepatocellular carcinoma; Aurora B kinase; AZD1152; Orthotopic model; Molecular-targeted agent.

Received 9 April 2009; received in revised form 2 July 2009; accepted 13 July 2009; available online 29 October 2009

\*Corresponding author. Tel.: +81 3 58035928; fax: +81 3 58035264.

E-mail address: shinji.msrg@tmd.ac.jp (S. Tanaka).

**Abbreviations:** cCasp-3, cleaved caspase-3; HE, hematoxylin and eosin; HCC, hepatocellular carcinoma; HQPA, hydroxyquinazoline-pyrazol-anilide; IC<sub>50</sub>, half-maximal inhibitory concentration; PBS, phosphate-buffered saline; PhH3, phosphohistone H3.

[1], and the incidence is still increasing [2]. The primary curative treatment for HCC is surgical resection, and there has been limited improvement in the availability of alternative treatments in the last decade [3]. A major obstacle for the treatment of HCC is the high frequency of tumor recurrence after curative resection. In fact, it is the recurrence pattern, rather than the recurrence itself, that critically affects patient prognosis [4]. The systemic treatment of HCC using conventional anticancer agents has provided little clinical benefit or prolonged survival for patients with advanced HCC [5]. A recent clinical trial by Llovet et al. [6] revealed a molecular-targeted inhibitor, sorafenib, as the first agent that demonstrated an improved overall survival in patients with advanced HCC. The increased understanding of the molecular mechanisms regulating cancer progression has led to the development of novel targeted therapies [7,8]. In order to fulfill this promise, there is an urgent need to identify the optimal targets for treatment.

In our previous studies in HCC patients after curative resection, the aggressive recurrence exceeding Milan criteria showed extremely poor prognosis [9]; moreover, a genome wide microarray profiling analysis identified the over-expression of Aurora B kinase as the only independent factor predictive of the aggressive recurrence [10]. The Aurora kinase family of serine-threonine kinases control chromosome assembly and segregation during mitosis. Aberrant expression of the Aurora kinases has been reported in a variety of solid tumors including prostate [11], colon [12], pancreas [13], lung [14], breast [15], and thyroid [16]. These findings have led to an interest in these kinases as molecular targets for cancer treatment [17,18]. Several small-molecule inhibitors of Aurora kinases have been developed as potential anticancer treatments. According to the recent review on Aurora inhibitors [19], ZM447439, Hesperadin, and MK0457/VX680 were the first to be described and to have similar potency versus Aurora A, Aurora B, and Aurora C. Currently, MLN8054 and MLN8237 are being developed as selective Aurora A kinase inhibitors. AZD1152 is a selective inhibitor of Aurora kinase activity with specificity for Aurora B kinase [20,21]. AZD1152 is a prodrug that is rapidly converted to the active moiety AZD1152-hydroxyquinazoline-pyrazol-anilide (AZD1152-HQPA) in plasma. Thus, AZD1152 is used for *in vivo* studies, while AZD1152-HQPA is used for *in vitro* work.

The importance of the role of the organ microenvironment in cancer is being increasingly understood [22]. This is particularly true for HCC, an organotrophic cancer in which the liver-specific



## Research Article

microenvironment may play a critical role in HCC tumor development, cellular apoptosis, and drug sensitivity [23]. Additionally, hepatic tumors reside within the liver parenchyma, where drug metabolism and transformation occur. Thus, the pharmacodynamics of drug therapy for intrahepatic tumors may vary significantly from those drugs targeted at tumors in peripheral tissues. Several attempts have been made to generate a model of intrahepatic HCC via intraportal or intrahepatic injection of tumor cells in mice; however, frequent cancer dissemination makes it particularly difficult to generate a single quantitative tumor. A recent report describes development of a novel orthotopic liver tumor xenograft model that could be used in quantitative investigations of a single tumor within its native microenvironment [24]. This might provide a system in which the tumor's biological response to therapeutic agents more closely mimics that observed in liver tumors in patients [25]. The *in vivo* efficacy of Aurora kinase inhibitors in orthotopic xenograft models of solid cancers has not been reported to date [20,26,27].

Outcome of HCC patients is determined by combination of two distinct types of HCC recurrence, and the aggressive recurrence is driven by malignant characteristics of the tumor [4,9]. Because Aurora B kinase was found to be associated with the aggressive recurrence exceeding Milan criteria [10], it makes sense to target Aurora B kinase to treat the tumor. In this regard, the Aurora B kinase-specific inhibitor AZD1152 might be an attractive candidate for HCC therapy. This investigation evaluates the *in vitro* and *in vivo* effects and pharmacodynamics of AZD1152 in a number of preclinical liver tumor models, including an orthotopic model that more closely mimics the human disease.

### Materials and methods

#### Reagents

AZD1152-HQPA and its prodrug AZD1152 were provided by AstraZeneca Pharmaceuticals (Macclesfield, UK).

#### Cell culture

The human HCC cell lines SK-Hep1, Hep3B, and PLC/PRF/5 were obtained from the American Type Culture Collection (Manassas, VA, USA). Other human HCC cell lines—JHH-1, JHH-2, JHH-4, HuH-1, HuH-6, HuH-7, HLE, HLF, and HepG2—were obtained from the Human Science Research Resources Bank (Osaka, Japan). Culture media were RPMI-1640 (SK-Hep1, Hep3B, HuH-7, and HepG2), Dulbecco's modified Eagle's medium (PLC/PRF/5, HuH-1, HuH-6, HLE, and HLF), and William's E medium (JHH-1, JHH-2, and JHH-4), supplemented with 5% fetal bovine serum (FBS) for HLF cells or 10% FBS for the remaining cell lines. All media supplemented 100 U/mL of penicillin and 100 µg/mL of streptomycin; all cell lines were cultivated in a humidified incubator at 37 °C in 5% carbon dioxide and harvested with 0.25% trypsin–0.03% EDTA.

#### Analysis of cell proliferation and cell viability

All cell lines were cultured in logarithmic growth phase in the presence of various concentrations of AZD1152-HQPA (0.3–1000 nM) for 72 h. Cells were seeded at  $4 \times 10^4$  cells in six-well plates with the appropriate control medium. After 24 h, plates were treated with compound and incubated for 72 h at 37 °C. At the end of the incubation time, cells were detached from each plate, and viable cells were counted using a hemocytometer. Half-maximal inhibitory concentration (IC<sub>50</sub>) values were calculated with BioDataFit v.1.02 software using the four-parameter logistic model. The mean values and standard deviations of IC<sub>50</sub> were calculated in triplicate for each cell line. To investigate cell viability, triplicate samples of SK-Hep1, Hep3B, and HLF cells were cultured in the presence of various concentrations of AZD1152-HQPA (1–100 nM) for 72 h. The number of nonviable cells was assessed using a hemocytometer and trypan blue dye exclusion.

#### Western blotting

Total protein was extracted from each cell line, as described previously [28]. Protein levels of Aurora B kinase, phosphohistone H3 (PhH3), and alpha-tubulin (control) were detected using standard western blot analysis on 8–15% sodium dodecyl sulfate polyacrylamide gel electrophoresis (SDS-PAGE). Blots were incubated overnight at 4 °C with the primary antibody antihuman Aurora B (1:1000; Abcam, Cambridge, UK; Catalog No. ab2254) or antihuman PhH3 (1:200; Santa Cruz, CA, USA; Catalog No. sc-8656-R), then at room temperature for 1 h with anti-alpha-tubulin (1:5000; Sigma-Aldrich, St. Louis, MO, USA; Catalog No. T9026). Appropriate secondary antibodies were added for 2 h, and protein expression was visualized with enhanced chemiluminescence by the ECL western blotting detection system (GE Healthcare, Buckinghamshire, UK). The expression ratio of Aurora B kinase to the control was analyzed using Multi-Gage software (FUJIFILM, Tokyo, Japan).

#### Flow cytometry

Samples of all cell lines in logarithmic growth phase were exposed to AZD1152-HQPA 100 nM for 24 h, and then fixed in 70% ethanol at –20 °C overnight. Cells were rehydrated in phosphate-buffered saline (PBS), and then resuspended in PBS containing RNase 100 µg/mL (Sigma) and propidium iodide 10 µg/mL. Cellular DNA content was analyzed on a FACS Caliber flow cytometer (Becton & Dickinson Biosciences, San Jose, CA, USA). For detection of apoptosis, cells were labeled with the Annexin V-FITC Kit (Mitenyi Biotec, Bergisch Gladbach, Germany; Catalog No. 130-092-052) at room temperature for 15 min, followed by analysis on a FACS Caliber flow cytometer.

#### Immunocytochemistry and immunohistochemistry

SK-Hep1, Hep3B, and HLF cells were cultured on glass slides coated with silane in the presence of various concentrations of AZD1152-HQPA (1–100 nM) for 4 h. They were then fixed using 3.7% formalin for 10 min and permeabilized using 100% methanol for 20 min for immunocytochemical detection of PhH3.

Xenograft tumor tissue was harvested, formalin fixed, and paraffin embedded. The primary antibodies, PhH3 (Upstate Cell Signaling Solution, Danvers, MA, USA; Catalog No. 9701) and anti-cleaved caspase-3 (anti-cCasp-3; Upstate Cell Signaling Solution; Catalog No. 9661), were used at 1:100 and 1:400 dilution, respectively, in PBS containing 1% bovine serum albumin. The tissue sections and slides were stained with an automated immunostainer (BenchMark XT; Ventana Medical Systems, Tucson, AZ, USA) using heat-induced epitope retrieval and a standard diaminobenzidine detection kit (Ventana).

#### *In vivo* studies in a subcutaneous tumor xenograft model

A subcutaneous tumor model was used to analyze the *in vivo* activity of AZD1152, as described previously [29]. Five-week-old female nude mice (nu/nu) were purchased from Japan SLC (Shizuoka, Japan) and kept under pathogen-free conditions, fed standard food, and given free access to sterilized water. In all experiments, mice were anesthetized by 100 mg/kg Nembutal intraperitoneal injection. Subcutaneous xenografts were established by inoculating  $1 \times 10^7$  SK-Hep1 cells into the right dorsal flank. Palpable tumors were confirmed on day 5 following inoculation, and mice were randomized into treatment groups to receive AZD1152 or the control Tris-buffered saline. AZD1152 was prepared in Tris-buffered saline (pH 9) and administered by intraperitoneal injection. Tumor size was measured using calipers as frequently as every other day for 2 weeks, and tumor volumes were calculated as  $AB^2 \times 0.5$  (A, length; B, width). The Animal Care Committee of Tokyo Medical and Dental University School of Medicine approved the experimental protocols in accordance with its institutional guidelines.

#### *In vivo* studies in a novel orthotopic xenograft model

An orthotopic xenograft model was created by direct intrahepatic inoculation of SK-Hep1 and Hep3B cells, as described by Lu et al. [25]. With the mice fully anesthetized, a small transverse incision was made below the sternum to expose the liver. Then,  $2.5 \times 10^6$  cells suspended in 25 µL of RPMI-1640 and 25 µL of Matrigel (Becton & Dickinson Biosciences) were slowly injected at a 30° angle into the upper left lobe of the liver using a 28-gauge needle. After injection, a small piece of sterile gauze was placed on the injection site, and light pressure was applied for 1 min to prevent bleeding. The abdomen was then closed with a 6–0 silk suture. Pilot studies confirmed development of liver tumors in 6 of 6 mice at